J Civil Struct Health Monit (2014) 4:277–288
DOI 10.1007/s13349-014-0086-3

ORIGINAL PAPER

Calibration of dielectric based moisture sensing in stone, mortar and stone-mortar sandwiches

J. H. Zhao · D. J. Thomson · E. Murison · G. J. van Rijn · A. De Mey · G. Mustapha

Received: 7 May 2014 / Revised: 5 July 2014 / Accepted: 8 July 2014 / Published online: 20 September 2014

Abstract Capacitance sensors with a capacitive sensing electronics have been calibrated for measuring moisture content (MC) in masonry stones. A total of 64 samples were tested. The MCs determined by gravimetry are correlated to the signals measured by the capacitive sensing electronics. The relationship between the MC and the measured voltage has been modeled using the linear least square regression along with error analysis. The results for the mortar and stone only specimens show the MC versus the voltage can be mathematically modeled by a linear equation with temperature-dependent fitting parameters. For the capacitance sensors in the mortar slots between two stones, the linear model was applied in the high MC and the low MC range, respectively, and two sets of linear equations with temperature-dependent fitting parameters have been established. The measurement with a higher MC shows stronger temperature influence that indicates necessity of temperature correction. The error estimations suggest the MC measurement be very likely affected with the variability of test samples. The sensors are best calibrated individually with the material of same type intended for the MC measurement.

Keywords Capacitance sensor calibrations · Moisture content (MC) · Gravimetric · Masonry stones

J. H. Zhao · D. J. Thomson (✉)
Department of Electrical and Computer Engineering, University of Manitoba, Winnipeg, Canada
e-mail: thomson@ee.umanitoba.ca

J. H. Zhao · D. J. Thomson
ISIS Canada Resource Center, University of Manitoba, Winnipeg, Canada

E. Murison
Water Management and Structures Division, Manitoba Infrastructure and Transportation, Winnipeg, Canada

G. J. van Rijn · A. De Mey
Heritage Conservation Directorate, PWGSC, Gatineau, Canada

G. Mustapha
SMT Research Ltd, Vancouver, BC, Canada

1 Introduction

Excessive accumulation of moisture often causes decay, corrosion and spalling of structural materials, leading to structural damage, functional degradation and microbial growth. The quantitative assessment of moisture (water) content (MC) in building materials is required for monitoring and predicting its impact on structural health. Instruments for measuring MC are often material specific and there is a growing need for simple low-cost sensors that can be deployed in wireless sensor networks. Therefore, there continues to be efforts to develop instruments for both academic and industrial needs in measuring, managing and controlling MC. There is particular interest in those capable of continuous moisture determination in the field [1, 2].

MC measurements are usually aimed at determining either the volume fraction or mass fraction of water (moisture) contained in a material. The MC of a material is normally referred to water molecules that have entered the material from external sources or environment in the form of so-called free water or exchangeable water [3]. The volumetric method measures the MC assuming a heterogeneous spatial distribution; the gravimetric method determines the MC by weighing the mass loss of a moist material during the drying, which is independent of the spatial distribution of moisture. Both methodologies

become equivalent under the circumstance of a homogeneous moisture distribution. The gravimetric determination of the MC has been standardized in many circumstances and is outlined in ASTM standards (D2216-10) [3]. This method does not apply to the in situ moisture measurement since it is destructive and cannot be practically implemented in situ.

Field system MC instruments usually make use of indirect measurements. Indirect MC measurement instruments measure the MC through detecting variation of material properties that are induced by the moisture. A number of approaches for MC measurement have been explored. These methods including thermography, ultrasound, nuclear magnetic resonance and neutron scattering are principally not based on electrical properties; the related instruments are relatively expensive, cumbersome and mostly used in laboratory [4].

Water has a high dielectric constant ($\varepsilon_r = 80$) and its presence will increase the overall dielectric constant of masonry materials ($\varepsilon_r = 1$–5) [5, 6]. Dielectric permittivity directly reflects strength of dielectric response of a water/material mixture to an external electric field. The dielectric permittivity is, therefore, a function of MC and provides an indirect means to MC. The most basic and popular method is to measure capacitance, where the material of interest acts as a dielectric medium between the electrodes of the capacitor. The capacitance is proportional to the dielectric constant of the dielectric medium and, therefore, reflects the MC of the material.

A variety of dielectric-based instruments (m), especially microwave based, are widely used for MC measurement, for example, in the fields of soil and bio-system [7–9]. However, they are difficult to apply universally and the in situ measurement often encounters great challenges due to large variability in materials. As to the effective MC measurement in complex masonry materials, the instrumental development is still not able to meet various needs encountered by practitioners in this field [1, 10]. The work reported in this paper is an effort made towards providing a tool for monitoring moisture in masonry walls.

In this work a simple dielectric technique to measure MC in masonry systems and a comprehensive calibration is presented. The project stemmed from the problems observed in accurately monitoring the moisture in the masonry walls, particularly in conservation of heritage structures [1]. Our previous studies led to the conclusion that dielectric-based capacitance sensing is an appropriate method to monitoring the MC level in stone [11]. As a result of that work a capacitance-sensing circuit working at 5 MHz frequency was designed by us for the MC measurement in the stone walls. In this work the sensing circuit is calibrated with respect to the MC by weight in test stone specimens. The advantage of using the capacitance-sensing circuit is that it is capable of in situ continuous measurement and can be easily integrated with data logging systems, especially wireless data logging systems. In addition, the sensing system is inexpensive. Thus, the calibrated wireless sensing system will be effective for MC monitoring in masonry structures.

2 Delectric capacitance sensors

The measurement of dielectric permittivity by the capacitance method relies on the adequate coupling of the sensor potentials into dielectric medium of the material of interest. In this work, capacitors are geometrically designed to be installed in a masonry wall. The capacitors have parallel electrodes in a same plane, as shown in Fig. 1, where one capacitor consists of two separated parallel metal conductors as in (b), called the TWIN-tape capacitance sensor; and another one is made in a form of the interdigitated arrays (IDA sensor) as in (c). Unlike a parallel-plate capacitor, where the field is confined between the plates, the two planar capacitors couple to the material of interest through a fringing electric field, as schematically shown in

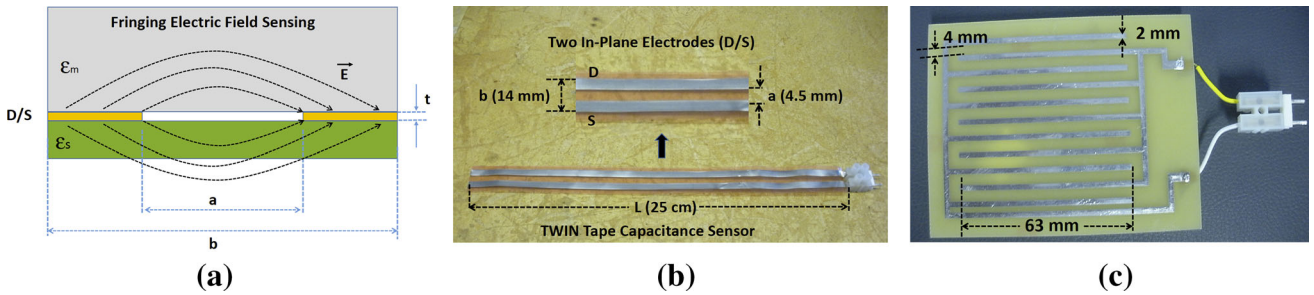

Fig. 1 Schematic of the capacitor with planer electrodes and the dielectric material (ε_m) as in (**a**), the TWIN tape capacitance sensor as in (**b**), and the IDA capacitance sensor as in (**c**)

Fig. 1a. When the masonry material is in contact with the metal electrodes, the electric field passes through the material, which acts as the dielectric medium in the capacitor. In Fig. 1a the material on the top of two electrodes (*D*/*S*) is assumed to be the masonry stone with a dielectric constant ε_m, and the dielectric material of ε_s is assumed to be the substrate of the sensing electrodes. Their capacitances can be calculated based on the following formula [12]:

$$C(DS) = \varepsilon_0\left(\frac{\varepsilon_m + \varepsilon_s}{2}\right)\kappa\left(\sqrt{1-\frac{a^2}{b^2}}\right)/\kappa\left(\frac{a}{b}\right) + \varepsilon_0\,\varepsilon_a\frac{t}{a} \quad (1)$$

where $\kappa\left(\sqrt{1-\frac{a^2}{b^2}}\right)$ and $\kappa\left(\frac{a}{b}\right)$ are the elliptical integrals.

The TWIN-tape sensor has a tape substrate of thickness of 0.3 mm and its other dimensions are shown in Fig. 1b; its calculated capacitance in air is approximately 2.80 pF and the measured value is about 2.84 pF @10 MHz (2.92 pF @ 100 kHz) using an impedance analyzer (Agilent 4294a). The IDA capacitor is constructed on a FR4 print circuit board which has a typical thickness of 1.5 mm and a dielectric constant ε_s of 4.35. The electrodes has a thickness t of about 35–100 μm. The capacitance of the IDA capacitor (with no coating layer on the electrodes) in air is approximately calculated as 13.0 pF and the measured value is 11.8 pF @10 MHz (12.0 pF @ 100 kHz).

The capacitance C (*DS*) is a function of the dielectric constant ε_m of the material. Variation of the ε_m thus can be detected by measuring the capacitance.

3 Capacitive interface electronics

Capacitance measurement can be made using a variety of electrical instruments, including commercial *LCR* meters and Impedance Analyzers often used in a laboratory. High performance instruments make use of advanced "bridge balance" techniques. They can achieve high accuracy and dynamic range, but are very expensive and bulky. There also are various handheld capacitance meters, which are relatively inexpensive, but their measurement capabilities are much more limited than those of the impedance analyzer. However, neither of these is suitable for widespread monitoring in applications such as wireless sensor systems. There are many capacitance measurement circuits that can be designed and made for various applications, including 'switch-capacitor based technique' [13], 'Relaxation oscillator circuit' technique [14] and phase differential detection method' [15]. In particular, modern integrated circuit (IC) technology is capable of mass producing versatile microcontrollers for capacitance measurement at a very low cost and small size [16]. Also, they can be easily integrated with wireless IC chips, offering advantages in the field of structural health monitoring [17, 18].

With a variety of capacitance-sensing technologies available, an appropriate choice is prerequisite for moisture measurement. In the accurate dielectric capacitance measurement of moisture the measuring frequency of the applied electric field is critical. Lower frequencies (less than 1 MHz) are dominated by the response of ions contained in the water. Higher frequencies (greater than 10 MHz) are technologically much more challenging. It was found that a sensing frequency of 5 MHz is capable of giving output signals well correlated to the gravimetric MC (wt%) of the stones. The lower working frequency makes LCR handheld meters and microcontroller capacitance sensors poor for moisture capacitance measurement in stone. Therefore, we have designed a simple 5 MHz capacitance-sensing electronics customized to this application and electrode geometry.

The capacitance-sensing circuit was based on comparing the charging time of a sensing and reference '*RC*' circuit. The '*RC*' circuit outputs an electric signal that changes in phase and amplitude with the variation of the capacitance. In the circuit schematic shown in Fig. 2a, the 'RC_s" is the capacitance sensing side, and the 'RC_r' is the reference capacitance circuit where C_r is a fixed capacitor. An electronic pulse with a width that depends on the '*RC*' of the sensing circuit is produced. After low-pass filtering with a capacitor, two output voltages V_a and V_b, are produced. The voltage V_a stemming from the 'RC_r' circuit is stable; the V_b from the 'RC_s" circuit changes with the sensing capacitance C_s. The difference between V_a and V_b is a measure of the capacitance variation of the sensing capacitor (C_s). The sensing circuit is shown in Fig. 2b along with a wireless data logger. The voltages of V_a and V_b from the sensing circuit are captured by the data logger and converted to digital data via an analog–digital (AD) converter; the digital data are then processed and wirelessly transferred to a computer.

The variation of the voltage difference ($V_1 = V_a - V_b$) is related to the change of the MC. Figure 2c shows the sensing circuit box with a half meter RF cable. The RF cable is used to connect the sensing circuit to the TWIN-tape capacitance sensor which is intended to be embedded in the stone wall where the capacitance of the TWIN-tape sensor will change with the MC. Commercial capacitors with a range of values were used to calibrate the sensing circuit. The voltage signal V_1 was measured with added capacitors in parallel with the TWIN-tape sensor. The measured voltage V_1 plotted against the added capacitance C (add) is shown in Fig. 3a, where measurement uncertainty of V_1 is approximately 2 mV. The change in V_1 with capacitance is nearly linear. The temperature sensitivity of the sensing circuit was tested from 10 to 40 °C and is shown in Fig. 3b. The results clearly show that the V_1 is

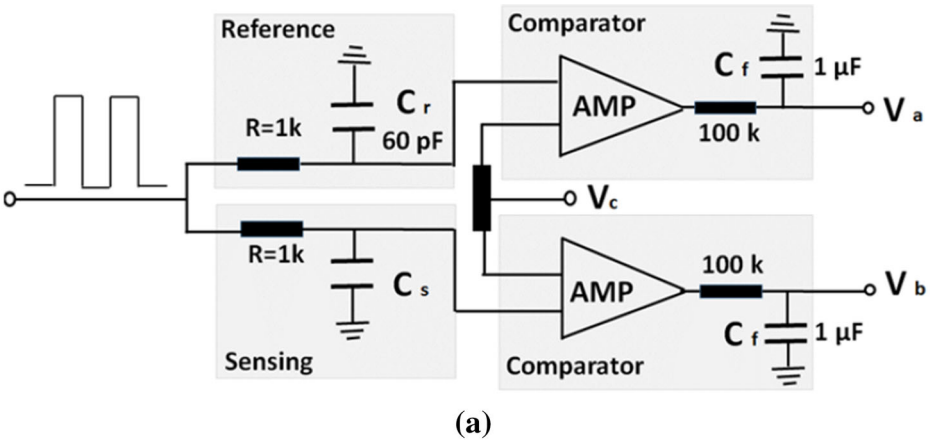

(a)

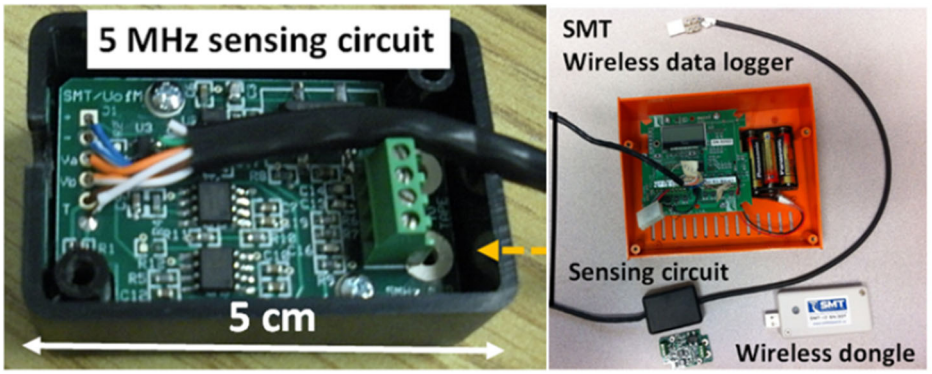

(b)

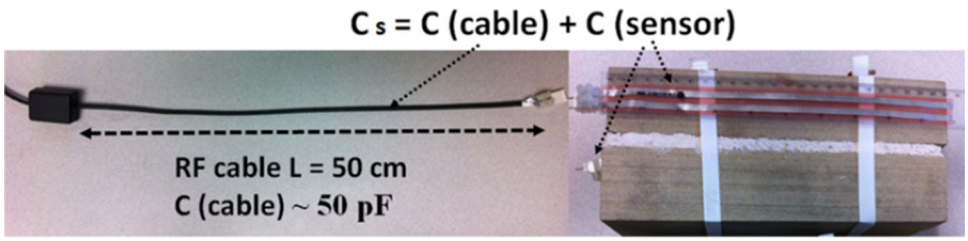

(c)

Fig. 2 The schematic diagram of the 5-MHz sensing circuit as in (**a**), the fabricated sensing electronics along with a wireless data logger system as in (**b**), the RF cable integrated TWIN-Tape capacitance sensor is in (**c**)

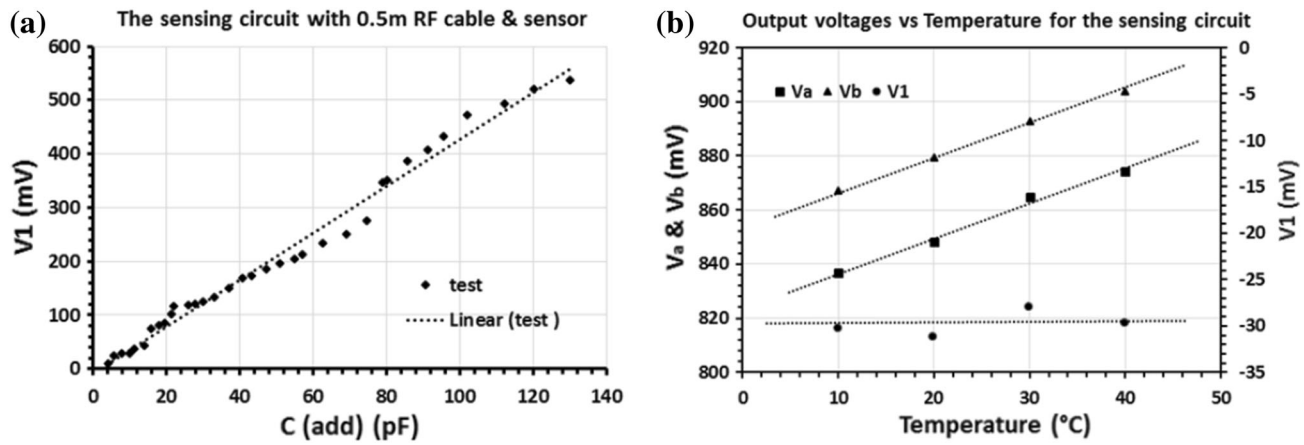

Fig. 3 **a** Calibration test results for the 5 MHz sensing circuit, **b** its temperature stability

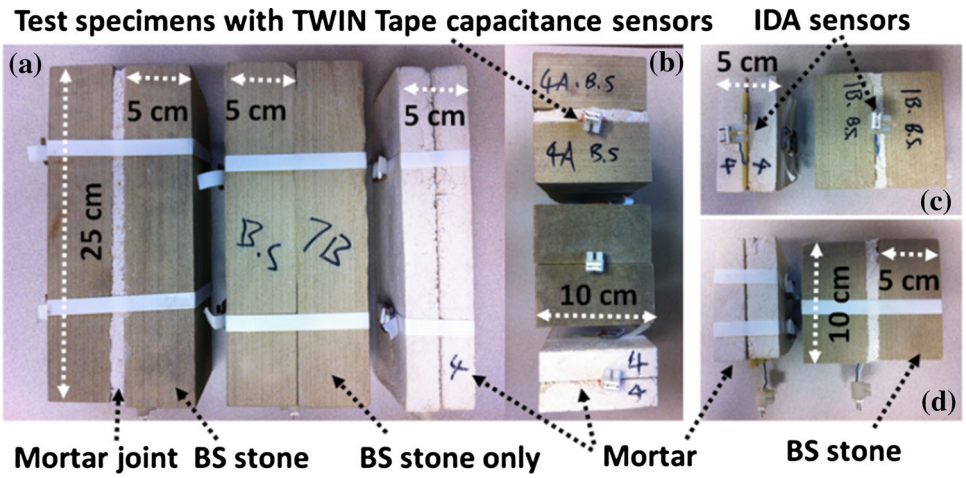

Fig. 4 Examples of the prepared test specimens (mortar and BS stone) with the sensors installed. Samples are held together with a fiberglass tape. The mortar appears as a *light colored* band

almost independent of temperature variation, with a maximum variation of 2 mV over this temperature range. The differential voltage is quite insensitive despite the V_a and V_b increasing linearly at 1.25 mV/°C.

4 Test specimen preparation and moisture saturation

Three types of stone, the Berea sandstone (BS), the St. Canut sandstone (STC) and the St. Marc limestone (STML), were selected for MC calibration. Mortar slabs were also prepared for testing. All stones were cut into two sizes of slabs to prepare specimens. The stone blocks with dimensions of $5 \times 10 \times 10$ (cm^3) were used to make sensor instrumented samples using the IDA capacitance sensors; the stone blocks with dimensions of $5 \times 10 \times 25$ (cm^3) were used for the TWIN-Tape sensor instrumented samples. The mortar slabs were moulded into two sizes: $2.5 \times 10 \times 25$ (cm^3) for the TWIN-tape sensor and $2.5 \times 10 \times 10$ (cm^3) for the IDA sensor, respectively. As shown in Fig. 4, the mortar test samples were prepared by tightly sandwiching the capacitance sensors between the two mortar slabs. The stone test samples were made in two formats: the one is the sensor is installed between two stone blocks together with an additional mortar layer of 0.5–1 cm acting as a bonding layer, where the side of the sensor electrodes is in direct contact with the surface of the stone and the other side of the sensor substrate contacts with the mortar; The Other one is the sensor is tightly sandwiched between the two stone blocks without bonding mortar. The mortar mix (1:2.5:8) was prepared by an experienced heritage mason (Parks Canada, Lower Fort Garry). The mix is composed of 1 part white Portland cement, 2.5 parts hydrated lime (type SA) and 8 parts sand. The mortar-bonded stone samples were made to simulate field installation. Fiber strapping tightly held all the test samples together.

The standard MC definition can be found in the ASTM standards as in ASTM D2216-10, where 'Standard Test Methods for Laboratory Determination of MC of Soil and Rock by Mass' is described in detail. The MC is defined as "the water extractable by oven drying at above boiling temperature until the moisture in the material has reached equilibrium". The MC is mathematically expressed and calculated by the following formula [3]:

$$MC(\text{wt}\%) = \frac{W_S(\text{moist}) - W_S(\text{dry})}{W_S(\text{dry})} \times 100\% = \frac{W(\text{mc})}{W_S(\text{dry})} \times 100\%$$

where W_s (moist) is weight of a moist specimen; W_s (dry) is weight of an oven dry specimen at 110 ± 5 °C; and W (mc) is weight of the absorbed water; MC (wt%) is the MC percentage by mass (gravimetric method). In this work, the MC measurement was carried out by directly measuring the sample weight using a weight scale (KERN 573-46NM), which has a maximum load of 6.5 kg and a resolution of 0.1 g.

The freshly made samples were put in the lab under a relative humidity (RH) of about 20 % and at a temperature of about 22 °C for a month until the mortar was cured and dried. The samples were submerged in deionized (DI) water to achieve saturation. Water absorption reached a saturation state when the measured weight did not change by more than ±0.5 g with time. The saturation state is reached by capillary saturation since water (moisture) permeation into the samples is predominated by the capillary transport [19]. The time to reach moisture saturation is different for each of the materials due to the differing diffusivity. The saturation time and the saturated MC for the prepared samples are listed in Table 1.

Table 1 Average moisture saturation MC (wt%) and saturation time for the sensor instrumented samples

Sensor instrumented specimens	Sample numbers	Average W_0 (g)	Average Ws (g)	Average W (mc) (g)	Average MC (wt%)	Saturation time
TWIN-Taper sensors with mortar	5	2165.9	2426.4	260.5	12.0	1 day
IDA sensor with mortar	5	912.7	1017.9	105.2	11.5	1 day
TWIN-Tape sensor/mortar bond BS	7	6048.4	6392.2	343.8	5.68	5 h
IDA sensor/mortar bond BS	5	2393.7	2525.4	131.2	5.50	5 h
TWIN-Tape sensor with BS only	3	5550.9	5856.2	305.4	5.50	5 h
TWIN-Tape sensor/mortar bond STC	6	7103.3	7227.3	124.0	1.75	2 days
IDA sensor/mortar bond STC	6	2764.6	2819.0	48.4	1.75	2 days
TWIN-Tape sensor with STC only	3	6652.9	6729.1	76.3	1.14	2 days
TWIN-Tape sensor/mortar bond STML	8	7533.0	7624.7	86.6	1.16	10 days
IDA sensor/mortar bond STML	6	2951.9	2977.7	25.9	0.89	10 days
TWIN-Tape sensor with STML only	3	6796.0	6813.0	16.9	0.25	10 days

Fig. 5 Testing setup for the MC sensor calibration in a RH/Temperature controllable chamber

5 Testing procedures for sensor calibration

5.1 Testing from MC saturation to dry at four temperatures

Calibration measurements were conducted in a RH/temperature controllable chamber as shown in Fig. 5. After the test samples were fully saturated, they were stored in sealed plastic bags to maintain a constant MC level during the test. At each testing temperature (40, 30, 20 and 10 °C) every sample was removed from the bag and quickly measured using the weight scale and the 5-MHz sensing circuit with the wireless data logger. After measurement, the samples were placed back in the bags and sealed to maintain the MC. The samples were held at each temperature for 18 h before testing. After completing a temperature sequence, the samples were taken out of their bags and exposed to the air in the chamber to dry out some of the moisture at 40 °C. Once the target weight of the samples, for example, corresponding to 80 % of the saturated MC, was reached, the samples were placed back in their bags and sealed to hold the obtained MC level for 3 days until a new equilibrium distribution of the MC in the samples was established. Equilibrium was established by monitoring the V_1 voltage. When it changed less than 2 mV over one day, equilibrium was assumed to have been reached. The temperature measurement sequence was then repeated for this new MC. This was repeated in roughly 20 % steps in MC until the samples reached near 0 % MC state.

5.2 Testing at four RH and four temperatures

After the samples were dried to a near 0 % MC state in the RH/temperature-controlled chamber, the relative humidity (RH)-dependent measurements were conducted at four temperatures of 40, 30, 20 and 10 °C, respectively. First, the RH was set to the lowest (5 %) in the chamber at the temperature of 40 °C for 2 weeks so that the MC in the samples were close to the target 0 % MC state. After that, all samples were measured at the temperature of 40 °C. Then, temperature was reset to the next lower value (i.e., 30 °C), stabilizing in about 2 h. The RH in the chamber was maintained for about 18 h at the new temperature, after which the measurements were repeated. This

procedure was followed until all measurements at four temperatures (40, 30, 20 and 10 °C) were completed for the fixed RH. Afterwards, a new RH (i.e., 25 %) in the chamber was set at 40 °C and maintained for 3 days so that a new moisture equilibrium state in the samples was achieved. All measurements for the MC weight and capacitance-sensing voltage were completed under four RH levels of 5, 25, 50 and 80 % at four temperatures.

6 Results and data analysis

Two types of capacitance sensors, the TWIN-Tape sensor and the IDA sensor, were tested with the 5-MHz sensing circuit to measure the MC in the mortar and stone specimens. The two types of capacitance sensors have the same working mechanism but differ only in electrode geometry and capacitance value, which resulted in very similar measurement results. Therefore, only the results for the TWIN-Tape sensor are presented and analyzed in this paper. Three types of the stones were tested for the MC calibration as shown in Table 1. The MC data show that the mortar and the BS stone specimens are the most permeable samples, as indicated by the higher saturated MC (MC wt%) and shorter saturation time. In contrast, the moisture absorption by the St. Canut sandstones is much less than that by the mortar and the Berea sandstones and takes more time to saturate. The St. Marc limestone has the lowest moisture diffusivity and the longest time for saturation and lowest percentage saturation MC. The calibration results are presented only with the mortar and the BS stone specimens. A large amount of calibration results for other types of stones and the IDA sensor are qualitatively similar and the detailed results will not be included in this paper.

6.1 Calibration results for mortar-only samples

Figure 6 shows the testing results of MC (wt%) versus V_1 (MC) at four temperatures for one of the mortar specimens with the TWIN-Tape capacitance sensor. The data show that MC (wt%) versus V_1 (MC) follows a linear relationship at each temperature. Therefore, a linear fit to the measured data is used to find calibration equations. The data at each temperature were mathematically fit using the least square regression method. The correlation coefficients (R^2) for the fit at 10°, 20°, 30° and 40° are 0.9873, 0.9944, 0.9962 and 0.9972, respectively. The fitted curves as shown in the dashed lines agree well with the measured data. In addition to the linear behavior, the measured data show that the measured voltage signals vary with the temperature for the same MC level. This temperature dependence becomes stronger when the MC is higher. The slopes and intercepts

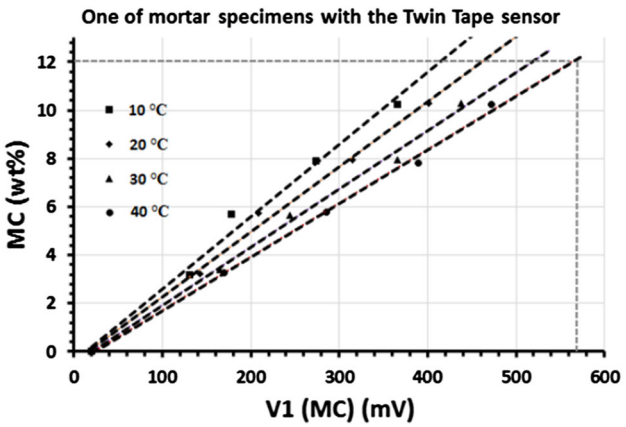

Fig. 6 The measured (*dots*) and fitted (*lines*) data for MC vs V_1 at four temperatures

Table 2 The fitting equations and uncertainty estimations for the mortar specimen

MC (wt%) = $a(T) \times V_1$ (mV) + $b(T)$	ΔMC = MC (predicted) – MC (measured)
$a(T) = -0.0003 \times T$ (°C) + 0.0323	±0.4 for (0 < MC < 12) (wt%)
$b(T) = -0.0043 \times T$ (°C) − 0.3447	

vary linearly with temperature. Consequently, the MC can be calculated from the voltage V_1 using a linear equation with the slope and intercept as a function of temperature. Table 2 gives these linear equations along with the error estimation ΔMC; ΔMC is the absolute uncertainty between the measured data and the calculated data from the equations, obtained by averaging errors for the data at each temperature using the least square regression method. In this case, the error is 0.4 % over the range of MC. In other words, MC changes greater than 0.4 % in a particular sample can be detected using the capacitive methods described.

Next, the measured data with a total of five mortar specimens will be processed in the same way as was done for a single sample described above. This analysis gives a calibration that includes the variability of the stone samples. In Fig. 7, the measured data from different specimens are plotted together against the measured MC. The data obtained at each temperature can be modeled using a linear curve. The scatter in the data are associated with variability of the test specimens due to either their natural properties or from sample preparations. Notwithstanding the scatter in the data, the whole set of data at each temperature still display a linear relationship between the measured voltages and the MC. Thus, a linear fit using the least square regression method was used to analyze the data at each

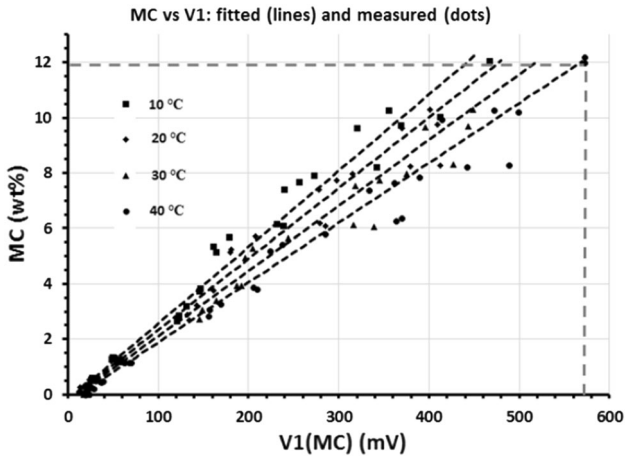

Fig. 7 The measured and fitted MC vs V_1 at four different temperatures for the mortar specimens

temperature. As seen above, the linear temperature-dependent slopes and intercepts were used to model the temperature dependence. The set of linear equations for calculating the MC from the measured voltage V_1 and their error estimates are shown in Table 3. The ΔMC indicates that the measurement at a MC higher than about 3 (wt%) would give a higher uncertainty of about 1 % (wt%). In comparison with the uncertainty of about 0.4 % (wt) for the individual specimen shown in Table 2, this larger error is mainly attributed to the variability of the specimens rather than the measurement itself. The error is lower at 0.4 wt% when the MC is less than 3 wt%. The measured data in the low MC range (less than 1.5 %) were taken from the RH-dependent measurements. The error estimate will be helpful to evaluate the measurement accuracy of the MC in the mortar specimens with the TWIN-tape capacitance sensor using the 5-MHz sensing circuit along with the wireless data logger.

6.2 Calibration results for the BS stone-only specimens

The measured data for three BS sandstone specimens at each temperature are shown in Fig. 8, where Fig. 8a shows the MC versus the voltage signal V_1 measured while the specimens were dried from 100 % saturated state to 0 %. Compared to the mortar specimens, the saturation MC (wt%) in these stone specimens is about 5.5 wt% and is lower than the saturated MC of 12 wt% in the mortar specimens. The measured voltage signal V_1 is accordingly lower corresponding to the lower MC. Similar to the mortar specimens, the temperature-induced difference in the measured voltage becomes larger in the higher MC range. The data at each temperature can be modeled using a linear relationship. The fitting equations of the MC versus V_1 and

Table 3 The fitting equations and uncertainty estimations for the mortar specimens

MC (wt%) = $a(T) \times V_1$ (mV) + $b(T)$	ΔMC = MC (predicted) – MC (measured)
$a(T) = -0.0002 \times T$ (°C) + 0.0296	±1.0 for (3 < MC < 12) (wt%)
$b(T) = -0.0026 \times T$ (°C) − 0.165	±0.4 for (0 < MC < 3) (wt%)

their temperature-dependent slopes and intercepts at each temperature were established using a linear least square regression, as shown in Table 4.

In addition to the results shown in Fig. 8a, b gives the measured data under four target RH conditions at four temperatures, where the MC range is below 0.3 % (wt%), i.e., below about 4.4 % of the saturation state. The measured MC versus V_1 in this low MC range is fit with a linear relationship, which was found to be different than the case where the MC was above this range. The corresponding temperature-dependent slopes and intercepts found in this low MC range are given in Table 4. The error analysis was done for the data in high and low MC ranges, respectively. The measurement in the lower MC range shows a much smaller absolute uncertainty.

6.3 Calibration results for the mortar-bonded BS stone specimens

Unlike the stone-only samples, the mortar-bonded specimens were prepared with a mortar joint between two slabs of stones and the capacitance sensor was installed between the stone and the mortar layer with the bare electrodes facing the stone. As shown in Fig. 9a, the voltage signal V_1 at the 100 % MC saturated state is higher than that for the stone-only specimens, as the higher MC in the mortar layer is partially detected by the sensor. As in the previous cases the voltage signal V_1 increases as temperature increases. The absolute voltage variation of the V_1 with temperature is smaller than that of the mortar specimens. The voltage V_1 decreases with the MC monotonically as expected. Different from the mortar specimens and the stone-only specimens, the voltage V_1 decreases slowly with the MC until the MC reduced down to about 20 % of the saturated state; after that, the voltage V_1 showed a quick drop with the MC decrease. It is obvious that the MC versus the voltage V_1 is not linear over the whole MC range. Thus, a linear fit to the entire range of the MC is not reasonable.

With several mathematical fitting models being considered, the most reasonable one was chosen for linearly fitting the data in two MC regions, higher or lower than approximately 20 % of fully saturated condition (1 % MC by wt%), respectively. Thus, the linear fit procedures

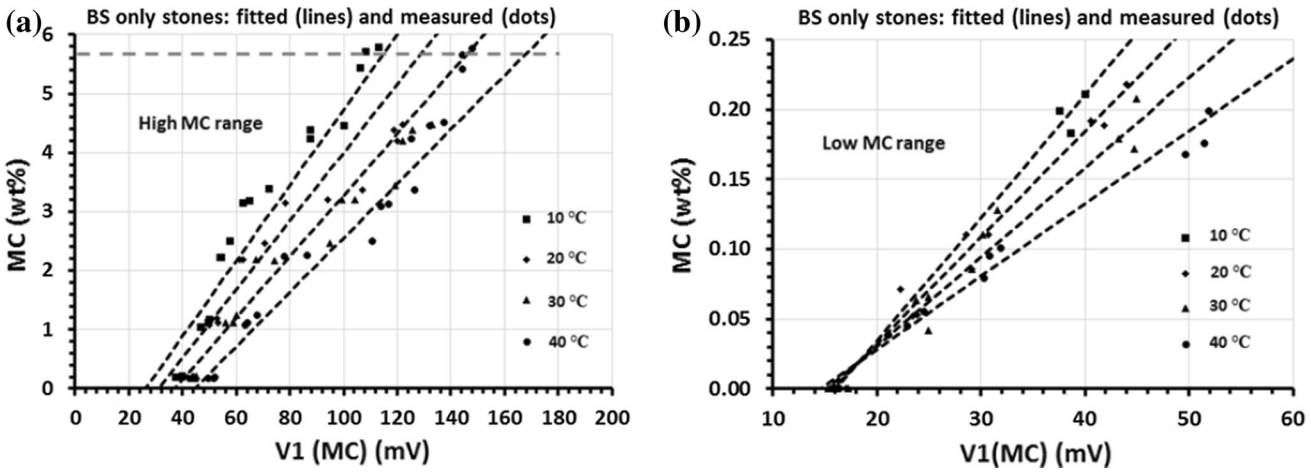

Fig. 8 The measured and its fitted MC vs V_1 at four temperatures in the high MC range (**a**) and low MC range (**b**) for the BS stone only specimens. The reported deviations are the maximum deviations from the fitted line and the measured results

Table 4 The fitting equations and uncertainty estimations for the BS stones only samples

MC (wt%) $= a(T) \times V_1$(mV) $+ b(T)$	ΔMC = MC (predicted) − MC (measured)
When $0.3 <$ MC < 5.5 (wt%)	When $0.3 <$ MC < 5.5 (wt%)
$a(T) = -0.0006 \times T$ (°C) $+ 0.07$	± 1.0 (wt%)
$b(T) = -0.0124 \times T$ (°C) $- 1.5483$	
When $0 <$ MC < 0.3 (wt%)	When $0 <$ MC < 0.3 (wt%)
$a(T) = -0.00012 \times T$ (°C) $+ 0.01$	$\pm$ 0.02 (wt%)
$b(T) = 0.0022 \times T$ (°C) $- 0.1634$	

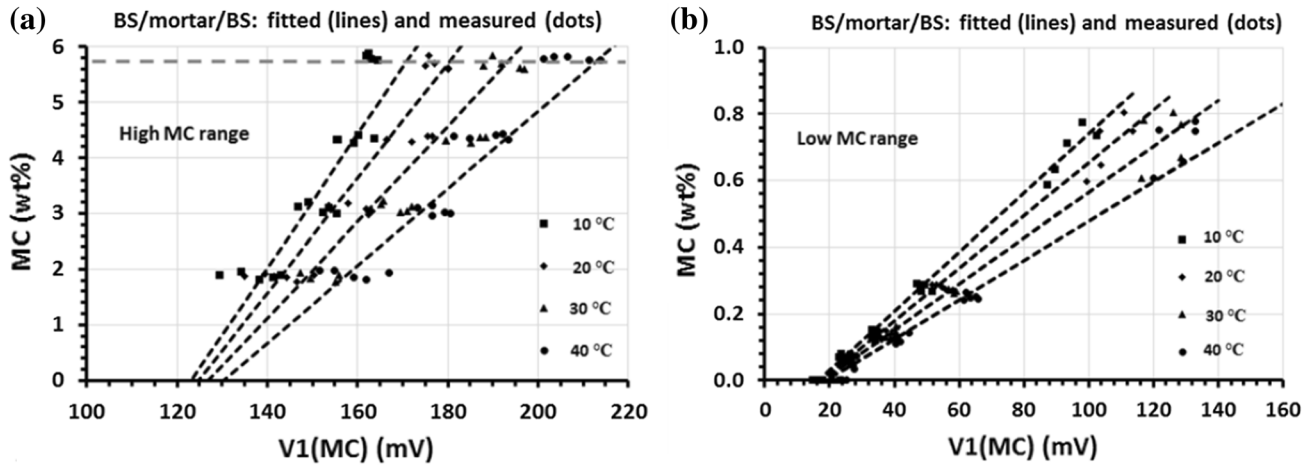

Fig. 9 The measured and fitted MC vs V_1 at four temperatures in the high MC range (**a**) and low MC range (**b**) for the mortar bonded BS specimens

described above were applied to the data in these two regions. As shown in Fig. 9a, the measured MC (wt%) versus V_1 (MC) was linearly fitted in the MC range above 1 % (wt%). The fitted data at four temperatures are shown as dashed lines, which are calculated from the fitting equations. It can be seen that the fitted lines match the measured data from the test specimens. Figure 9b shows the measured and the fitted data at the MC region less than 1 % (wt%). The data below the MC of 0.3 % (wt%) were measured at four temperatures under four different RH conditions in the chamber, where the MC (wt%) is the absorbed moisture corresponding to the specific RH. The MC data between 0.6 and 0.8 % (wt%) were taken from the measurement while drying from saturation. The fitting

Table 5 The fitting equations and error estimations for the mortar bonded BS stones

MC (wt%) = $a(T) \times V_1$ (mV) + $b(T)$	ΔMC = MC (predicted) − MC (measured)
When 1.0 < MC < 5.7 (wt%)	When 1.0 < MC < 5.7 (wt%)
$a(T) = -0.0017 \times T$ (°C) + 0.1375	±1.0 (wt%)
$b(T) = 0.1932 \times T$ (°C) − 16.786	
When 0 < MC < 1.0 (wt%)	When 0 < MC < 1.0 (wt%)
$a(T) = -0.0001 \times T$ (°C) + 0.0099	± 0.1 (wt%)
$b(T) = 0.0012 \times T$ (°C) − 0.1601	

equations in the high and low MC regions are summarized in Table 5 along with their error estimations. The measurement uncertainty in the low MC range is clearly lower than that in the high MC range.

7 Discussion

The work reported in this paper has focused on the calibration of a capacitive sensor for measuring the MC in masonry. The moisture sensor calibration involves two major physical phenomena: moisture storage and transport in the porous material and the dielectric properties of moist materials. We will discuss these to aid in the understanding and interpretations of the sensor calibration results.

Masonry materials are hygroscopic and mainly absorb moisture in air through vapor diffusion or absorb water by a capillary action in contact with liquid water [19]. Given sufficient time, an equilibrium moisture distribution in the materials will be eventually reached when the surrounding moisture condition is held at constant RH, temperature and pressure. In an environment with the RH from 0 % to about 95 %, a sorption isotherm curve under an isothermal equilibrium state is usually used to describe the moisture absorption behavior, which is often determined by gravimetric method [19, 20]. At near 100 % RH, moisture condensation occurs, leading to moisture on the surface of the materials and inducing the capillary moisture transport into the materials [19]. When in direct contact with liquid water, moisture (water) diffuses into the materials mainly through the capillary transport. Eventually, when the moisture reaches a saturated state, it is defined as capillary moisture saturation. Another kind of moisture saturation occurs when pressure is applied; it is called the vacuum saturation. The capillary saturation is normally less than the vacuum saturation [19]. In this work, the capillary saturation was employed for the sensor calibration as moisture saturation in the masonry walls mostly occurs through absorption from the ground or by direct surface water contact, such as rain. Due to the large variability of the material properties in porosity, structural compositions and the interplays with moisture, the moisture transport and storage properties in the materials can vary widely, as partially evidenced by the measurements on moisture saturation shown in Table 1.

Our calibrations were conducted by drying the specimens from the saturated state. The drying process is a reverse process of moisture absorption; it is described by desorption isotherm and characterized with a hysteresis curve with absorption isotherm [19, 21]. Moisture desorption is often much slower than the absorption. The driving forces and mechanisms for moisture desorption are different from those for the absorption due to the different boundary conditions for the moisture transport. The drying process involves moisture vapor and capillary diffusion as well as vapor evaporation. Moisture distribution during drying often shows a gradient profile [22, 23]. This is why our specimens were kept in the plastic bags for some time to achieve a new moisture equilibrium distribution state for the sensor calibration. Further detailed investigations on the moisture distributions in the samples would be helpful to understand more clearly the 'bi-linear' behavior in the high MC and low MC range for the mortar bonded BS stone specimens.

Capacitance sensors measure dielectric permittivity that is a function of the MC of the stone specimen. The dielectric contribution by water is assumed to be predominated by dipole orientation polarization in an electric field [24]. In porous material such as masonry, the dielectric response induced by water could become more complicated because the materials are composed of various chemical compositions and their structures are non-crystalline, heterogeneous and disordered. Water molecules in the pores exist in the form of vapor and liquid as a solution. The physical and electrochemical interactions between water and solid composite materials will result in an ion-containing solution, carrying electric charges. As a result, additional dielectric responses could be introduced with the ionic-carrying system, such as interfacial polarization (i.e., Maxwell–Wagner dielectric relaxation) and double-layer polarization [25–28]. The dielectric polarizations are dependent on both frequency and temperature [29, 30]. In particular, moisture-induced interfacial polarizations will be more significant at low frequencies and high temperatures. The additional dielectric responses will make their contributions to the dielectric permittivity measurement.

The measurement at a lower frequency will result in a higher dielectric permittivity. The dielectric permittivity will be greatly reduced when the higher measuring frequency is applied. This frequency-dependent characteristic should be taken into consideration when the moisture-sensing instruments are designed, especially, when the sensing instruments are calibrated with the porous materials containing moisture. The measuring frequency is best chosen so that the dielectric response can be well correlated to MC. Our studies on the frequency dependence of the capacitance measurement in the moist stones have led us to develop the capacitance sensing circuit working at 5 MHz. At this working frequency, the capacitance measured can be well correlated to the MC in the masonry stones. It is the dielectric characteristics in the low frequency that made the handheld *LCR* meters and microcontroller sensing electronics not suitable for MC measurement in stone. As to the many other moisture instruments based on microwave methods with much higher working frequencies for measuring the dielectric response, they are often more complicated and expensive than the sensing electronics used in this work. As presented in this work, the 5-MHz capacitance-sensing electronics can be easily integrated with wireless data loggers for the continuous measurement, along with additional advantages in small size, low cost and easy deployment in the masonry walls.

8 Summary

In this work, two types of dielectric-based capacitive sensors with specifically designed sensing electronics have been calibrated to measure the MC in building stone and building stone with mortar joints. The calibration tests were carried out by sequentially drying to four target MC levels from the 100 % saturated state at temperatures 10, 20, 30 and 40 °C, respectively. In addition, the calibrations were done after the MC was conditioned at four different relative humidity levels. The relationship between the MC (wt%) and the measured signal has been modeled using linear relationships. The measurement uncertainty was also given by least square error analysis.

The linear equations together with their temperature-dependent slopes and intercepts have been obtained for the mortar and stone only specimens. The MC in the mortar and the stones can be calculated from the measured voltage and temperature using the fitted linear equations. For the sensor calibrations with the mortar-bonded stones (mortar slots), the linear fit was used to model the relationship between the measured voltage and the MC (wt%) in two MC ranges: the high MC and the low MC ranges, where two sets of fitted linear equations have been established for the MC estimations from the measured voltages.

Temperature correction becomes more important at higher MC levels in the stones. The sensor calibration should be made for different types of masonry materials due to the variability of moisture behaviors and dielectric properties. For accurate application of the calibrated data, it is crucial to install the capacitance sensors such that they closely match the geometry of the calibration sensors and specimens.

With the demonstrated capability for measuring MC, practical applications of the developed moisture-sensing electronics will be further explored in in situ moisture monitoring in masonry walls and optimization of the sensing system.

Acknowledgments This work was contracted and financially supported by the Public Works and Government Services Canada. The Authors highly appreciate the SMT Research Ltd. for collaborations in fabricating the sensing electronics and providing a wireless data logger.

References

1. Camuffo D, Bertolin C (2012) Towards standardization of moisture content measurement in cultural heritage materials. Moisture content measurement in heritage materials. e-Preserv. Sci. 9:23–35
2. Phillipson MC, Baker PH, Davies M, Ye Z, McNaughtan A, Galbraith GH, McLean RC (2007) Moisture measurement in building materials: an overview of current methods and new approaches. Build Serv Eng Res 28(4):303–316
3. ASTM (D2216-10) Standard test methods for laboratory determination of moisture content (MC) of soil and rock by mass, p 7
4. Healy WM (2003) Moisture sensor technology—a summary of techniques for measuring moisture levels in building envelopes. ASHRAE Trans 109(1):232–242
5. Rusiniak L (1998) Dielectric constant of water in a porous rock medium. Phys Chem Earth 23:1133–1139
6. Knight R, Endres A (1990) A new concept in modeling the dielectric response of sandstones: defining a wetted rock and bulk water system. Geophysics 55(5):586–594
7. Muñoz-Carpena R, Shukla S, Morgan K (2004) Field devices for monitoring soil water content. BUL 343 (http://edis.ifas.ufl.edu/pdffiles/AE/AE26600.pdf)
8. Stacheder M, Koeniger F, Schuhmann R (2009) New dielectric sensors and sensing techniques for soil and snow moisture measurements. Sensors 9:2951–2967
9. Venkatesh MS, Raghavan GSV (2003) An overview of dielectric properties measuring techniques. Can Biosyst Eng 47: 7.15–7.30
10. Nady M, Saïd A (2007) Measurement methods of moisture in building envelopes—a literature review. Int J Archit Herit 1(3):293–310
11. Zhao JH, Rivera E, Mufti A, Stephenson D, Thomson DJ (2012) Evaluation of dielectric based and other methods for moisture content measurement in building stones. J Civil Struct Health Monit 2:137–148. doi:10.1007/s13349-012-0024-1
12. Dean RN, Rane A, Baginski M, Richard J, Hartzog Z, Elton DJ (2012) A capacitive fringing field sensor design for moisture measurement based on printed circuit board technology. IEEE Trans Instrum Meas 61:1105–1112
13. Heidary A, Meijer GCM (2007) A low-noise switched-capacitor front end for capacitive sensor. In: Conference on IEEE sensors 2007, pp 40–43

14. McIntosh RB, Casada ME (2008) Fringing field capacitance sensor for measuring the moisture content of agricultural commodities. IEEE Sens J 8(3):240–247
15. Majid HA, Razali N, Sulaiman MS, A'ain AK (2009) A capacitive sensor interface circuit based on phase differential method. World Acad Sci Eng Technol 3:593–596
16. Ferran R (2012) The art of directly interfacing sensors to microcontrollers. J Low Power Electron Appl 2:265–281. doi:10.3390/jlpea2040265
17. Lynch JPA (2007) An overview of wireless structural health monitoring for civil structures. Phil Trans R Soc 365:345–372
18. Thomson DJ, Card D, Bridges GE (2009) RF cavity passive wireless sensors with time-domain gating-based interrogation for SHM of civil structures. IEEE Sens J 9:1430–1438
19. Janz M (2000) Moisture transport and fixation in porous materials at high moisture levels. PhD thesis, Lund University, Sweden
20. Kumaran MK (1999) Moisture diffusivity of building materials from water absorption measurements. J Therm Envel Build Sci 22:349–355
21. Scheffler GA, Plagge R (2010) Introduction of a drying coefficient for building materials. ASHRAE, Buildings XI: 1–12
22. Rosenkilde A (2002) Moisture content profiles and surface phenomena during drying of wood. PhD thesis
23. Scheffler GA (2011) Application of instantaneous profile measurement of moisture content and moisture potential in porous materials. Mater Struct 44:1517–1536
24. Coffey WT, Kalmykov YP, Feldman Y, Puzenko A and Ryabov Y (2005) Dielectric relaxation phenomena in complex material. doi:10.1002/0471790265.ch1
25. Sen PN, Chew WC (1983) The frequency dependent dielectric and conductivity response of sedimentary rocks. J Microw Power 18(1):95–105
26. Howell BF, Licastro JRPH (1961) Dielectric behavior of rocks and minerals. The Am Mineral 46:269–288
27. Gomaa MM (2008) Relation between electric properties and water saturation for hematitic sandstone with frequency. Anal Geophys 51(5/6):801–811
28. Nover G (2005) Electrical properties of crustal and mantle rocks—a review of laboratory measurements and their explanation. Surv Geophys 26:593–651. doi:10.1007/s10712-005-1759-6
29. Hill NE (1970) The temperature dependence of the dielectric properties of water. J Phys C Solid State Phys. 3: 238–239. http://iopscience.iop.org/0022-3719/3/1/026
30. Liu CH, Zhang LB, Peng JH, Srinivasakannan C, Liu BG, Xia HY, Zhou JW, Xu L (2013) Temperature and moisture dependence of the dielectric properties of silica sand. J Microw Power Electromagn Energy 47(3):199–209